Biosensors and Bioelectronics 25 (2010) 1130–1136

Contents lists available at ScienceDirect

Biosensors and Bioelectronics

journal homepage: www.elsevier.com/locate/bios

Electrochemical immunosensor based on colloidal carbon sphere array

Xiaojun Chen[a,c], Kui Zhang[b], Jinjun Zhou[a], Jie Xuan[a], Wei Yan[a], Li-Ping Jiang[a,*], Jun-Jie Zhu[a,*]

[a] Key Lab of Analytical Chemistry for Life Science (MOE), School of Chemistry and Chemical Engineering, Nanjing University, Nanjing 210093, PR China
[b] The Affiliated Drum Tower Hospital of Nanjing University Medical School, Nanjing 210008, PR China
[c] College of Sciences, Nanjing University of Technology, Nanjing 210009, PR China

ARTICLE INFO

Article history:
Received 13 July 2009
Received in revised form
11 September 2009
Accepted 28 September 2009
Available online 7 October 2009

Keywords:
Colloidal carbon spheres array
Electrochemical impedance spectroscopy
Immunosensors
Immunoglobin A

ABSTRACT

A novel type of colloidal carbon sphere array (CSA) was developed for the fabrication of disposable electrochemical immunosensor. The CSA was successfully prepared on indium tin oxide (ITO) substrate in a simple manner and the scanning electron micrograph confirmed that a single-layered arrangement of the carbon spheres with its (1 1 1) plane paralleled the substrate's surface. The CSA modified electrode has a higher surface area and exhibits a more sensitive electrochemical response than a normal carbon-based electrode with the same geometric area. An Immunoglobin A (IgA) immunosensor was constructed by the covalent bonding of IgA antibody molecules with the CSA aided by large numbers of carboxyl groups on the surface of carbon spheres. The immunosensor exhibited a wide linear response to IgA ranging from 0.1 to 200 ng mL^{-1} by electrochemical impedance spectroscopy (EIS) technique. The detection of IgA levels in three sera obtained from hospital samples showed acceptable accuracy.

1. Introduction

Immunosensors that can transform specific antibody–antigen (Ab–Ag) interactions into measurable piezoelectric (Jin et al., 2009), acoustic (Krishnamoorthy et al., 2008), electrochemical (Fu, 2007), magnetic (Mani et al., 2009) and optical signals (Sanchez-Martinez et al., 2007; Fu et al., 2006), have been studied extensively for clinical diagnosis (Watterson et al., 2007), environmental pollutant detection (Gonzalez-Martinez et al., 1999) and food analysis (Zacco et al., 2007). Among them, electrochemical immunosensors have recently attracted considerable interest because of their relative simplicity, high sensitivity, low cost and inherent miniaturization (Lin and Ju, 2005; Marquette and Blum, 2006; Bakker and Qin, 2006). In recent years, great progress in nanoscience and nanotechnology has opened new opportunities for assembling electrochemical immunosensors. A variety of nanomaterials has been utilized to assist the fabrication of electrochemical immunosensors, including colloidal gold/silver, semiconductors, carbon or silica nanoparticles, and magnetic beads (Suni, 2008). Among these nanomaterials, novel carbon nanostructrues such as carbon nanotubes (CNT), carbon nanofibers (CNF) and carbon nanorods (CNR) are popular as the support materials for electrochemical immunosensors due to their electrical conductivity, large surface area, good chemical stability and excellent biocompatibility (Viswanathan et al., 2009; He et al., 2009; Wu et al., 2007; Wang and Lin, 2008; Cui et al., 2008a; Jie et al., 2008). Electrochemical biosensors modified with the carbon nanostructure onto the electrode surface are constructed mostly by drop coating method, resulting in an unknown spatial relationship between the immobilized biomolecule and the nanostructure. Random planar meshes of carbon nanostructures will decrease the density of functional groups on the electrode surface and hence the sensitivity of the biosensors. Thus, a highly oriented carbon nanostructure has been proposed as a possible ideal structure for the application in bioelectrochemical field.

A highly ordered CNT array was reported to serve as a universally direct nanoelectrode interface for the fabrication of a glucose oxidase biosensor (Withey et al., 2006). Another vertically aligned CNF chip was demonstrated as a sensing element for application of an electrochemical DNA sensor (Arumugam et al., 2009). Electron transfer has been enhanced markedly using these carbon array modified electrodes. Some other CNT or CNR arrays have been fabricated as promising platforms for biosensor development (Nguyen et al., 2002; Orikasa et al., 2009; Yun et al., 2008). However, it is not easy to control the array structures, such as orientation, length and diameter. The most commonly used methods for growing high ordered CNT or CNF arrays on substrate are the catalytically chemical vapor deposition (CVD) process (Yun et al., 2007; Maldonado and Stevenson, 2004) and the anodic aluminium oxide (AAO) template technique (Li et al., 1999; Rahman and Yang, 2003). However, these methods are tedious and time-consuming, and thus the fabrication of a carbon nanostructure array is appealing as a more convenient technique.

Herein, we introduced a novel type of colloidal carbon sphere array (CSA) as substrate to fabricate a sensitive IgA electrochem-

* Corresponding authors. Tel.: +86 25 83594976; fax: +86 25 83594976.
E-mail addresses: Jianglp@nju.edu.cn (L.-P. Jiang), jjzhu@nju.edu.cn (J.-J. Zhu).

0956-5663/$ – see front matter © 2009 Elsevier B.V. All rights reserved.
doi:10.1016/j.bios.2009.09.038

ical immunosensor. The monodisperse colloidal carbon spheres with narrow size distribution were prepared by a microwave-hydrothermal route in aqueous glucose solution. The as-prepared colloidal carbon spheres can not only maintain excellent characteristics as normal carbon materials, but also disperse well in water due to abundant hydrophilic oxygen-containing functional groups on their surfaces. The CSA modified indium tin oxides (ITO) electrode was fabricated with a simple vertical deposition technique, which was promising for mass production of the immunosensor. To the best of our knowledge, no reports were found about electrochemical immunosensors based on CSA modified electrode. In the fabrication of the sensor, Ab was bonded to the carbon spheres through the covalent combination of amino groups in the Ab and carboxyl on the carbon spheres. After residual unreacted active sites were blocked by bovine serum albumin (BSA), the IgA electrochemical impedance spectroscopy (EIS) immunosensor was developed, which exhibited a sensitive response to IgA with the lowest concentration of 0.1 ng mL^{-1}. The CSA can be further extended to other biological systems because it offers a cost-effective, versatile, and highly specific protocol in clinical diagnoses. The detailed optimization and performance characteristics of the developed immunosensor are reported in the following sections.

2. Experimental

2.1. Chemicals and materials

Glucose (analytical purity) was purchased from Beijing Chemical Reagent Factory. 1-Ethyl-3-(3-dimethylaminopropyl) carbodiimide hydrochloride (EDC), N-hydroxysuccinimide (NHS) and lyophilized 99% bovine serum albumin were obtained from Sigma/Aldrich. Human IgA and goat anti-human IgA (Ab) were purchased from Shanghai Kehua Bio-engineering Co., Ltd. (Shanghai, China). Human serum samples were obtained from the Affiliated Drum Tower Hospital of Nanjing University Medical School and used as received. All other reagents were of analytical reagent grade and used without further purification. Phosphate-buffered saline (PBS buffer, 50 mM, pH 7.4, 6.0 and 4.0) was prepared by mixing stock solutions of NaH_2PO_4 and Na_2HPO_4, and then adjusting the pH with 50 mM NaOH or H_3PO_4. The standard IgA solutions were prepared in the pH 6.0 PBS buffer solution, and the Ab and 3% BSA solutions were prepared in pH 4.0 PBS buffer and stored at 4 °C. Ultrapure fresh water obtained from a Millipore water purification system (MilliQ, specific resistivity > 18MΩ cm^{-1}, S.A. Molsheim, France) was used in all experiments. Indium tin oxides glass was purchased from Conduc Optics & Electronics Technology Co., Ltd. (Changzhou, China).

2.2. Apparatus

The microwave-assisted hydrothermal reaction was conducted in a microwave accelerated reaction system MARS-5 (CEM, USA). The size of the prepared monodispersed carbon colloidal spheres was determined by transmission electron microscopy (TEM, JEOLJEM-200CX) and a Brookhaven BI-9000AT laser dynamic light scattering (DLS) system (Brookhaven Instruments Corporation, USA). The morphology of CSA was verified by field-emission scanning electron microscopy (FESEM, HITACHI S4800). All Fourier-transform infrared (FTIR) spectroscopic measurements were performed on a Bruker model VECTOR22 Fourier-transform spectrometer using KBr pressed disks. Zeta potential analysis was performed with a PALS Zeta Potential Analyzer, Version 3.43 (Brookhaven Instruments Corp.). The electrochemical impedance measurements were carried out with an Autolab PGSTAT12 (Eco Chemie, BV, The Netherlands) and controlled by GPES 4.9 and FRA 4.9 software. Cyclic voltammetry measurements were performed on a CHI660B electrochemical workstation (Shanghai CH Instruments Co.). A conventional three-electrode system was used, comprising a platinum foil as the auxiliary electrode, a saturated calomel electrode (SCE) as the reference and a CSA modified electrode as the working electrode. All potentials herein are in reference to the SCE.

2.3. Preparation of monodisperse carbon colloidal spheres

Monodisperse carbon colloidal spheres with the diameter of ~300 nm (relative standard deviations 3.2%) were synthesized by a microwave-hydrothermal route as described in the previous report (Cui et al., 2008b). Briefly, 5 g of glucose was dissolved in 40 mL of water to form a clear solution, which was treated at 170 °C and 180 pounds per square inch (psi) for 20 min in a 50 mL reaction vessel lined with Teflon. The microwave-accelerated reaction system was operated at a power of 200 W. The coffee-brown products were washed with water and alcohol by six centrifugation/redispersion cycles and oven-dried at 70 °C.

2.4. Preparation of CSA modified electrodes

Firstly, ITO substrates were cleaned with acetone and EtOH in an ultrasonic bath for 10 min to remove any inorganic or organic contaminants on the substrate surface. The substrates were then rinsed thoroughly with ultrapure water and dried under nitrogen flow. The cleaned ITO substrate was vertically immersed into a vial containing 2 wt.% water suspension of carbon spheres and the apparatus was placed in a vibration-free temperature-controlled oven at 50 °C for about 48 h. After that, along with the evaporation of water, a CSA modified ITO was obtained. The electrode geometric area was controlled by an apertured insulating tape covering the edge of carbon sphere layer and was determined to be 0.07 cm^2.

2.5. Fabrication of the IgA immunosensor

The fabrication process of the sensor is shown in Scheme 1. The CSA modified ITO electrode was first immersed in a solution containing 20 mg mL^{-1} of EDC and 10 mg mL^{-1} of NHS at room temperature for 1 h to activate the carboxyl groups on the surface of the carbon spheres. After thoroughly rinsed with ultrapure water, it was soaked in a PBS solution of Ab at 4 °C overnight. In this way, the Ab was immobilized on the surface of the CSA modified ITO electrode to form Ab–CSA bioconjugates that can be used in immunoassay. Unbound antibodies were washed away with water. The unreacted covalent-active surface groups were subsequently blocked by reaction with 3% (w/w) BSA at room temperature for 2 h. After the electrode was rinsed with water three times, an IgA immunosensor was fabricated. When not in use, the sensor was stored in air at 4 °C.

2.6. Electrochemical measurements

The prepared IgA immunosensor was incubated in 400 μL of solution containing different concentrations of IgA at 37 °C for 30 min and washed carefully twice with water to obtain an immobilized bioconjugate layer. The amount of produced immunocomplex depended on IgA concentration in the standard sample solution. The EIS was recorded in the frequency range between 0.01 Hz and 1.0×10^5 Hz, at the formal potential of the $[Fe(CN)_6]^{3-/4-}$ redox couple and with a perturbation potential of 5 mV. The electrochemical measurements including CV and EIS were performed in a degassed pH 7.4 PBS solution with 0.1 M KCl and 2 mM $[Fe(CN)_6]^{3-/4-}$.

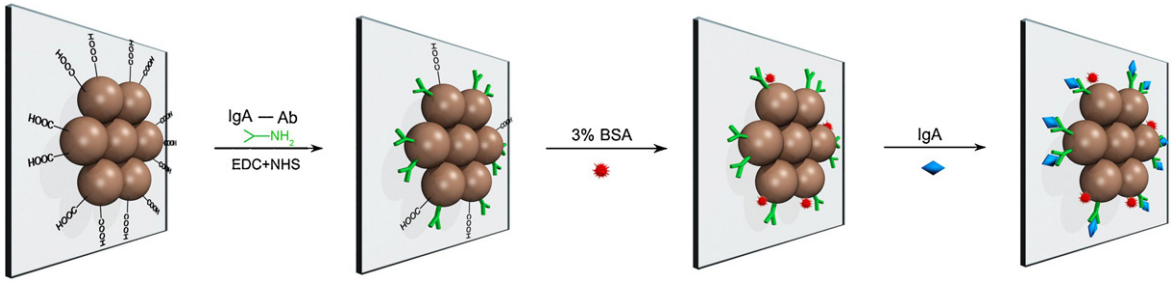

Scheme 1. Schematic illustration of the IgA immunosensor fabrication process.

The real serum samples were diluted to the appropriate concentrations from 10 to 50 ng mL^{-1} with pH 6.0 PBS buffer respectively. The data presented for condition optimization, and calibration curves was the average of 3 recorded measurements.

3. Results and discussion

3.1. Preparation of CSA

Carbon spheres were prepared from glucose under microwave-hydrothermal conditions at 170 °C, this higher-than-normal glycosidation temperature led to aromatization and carbonization (Luijkx et al., 1995; Wang et al., 2002). The FTIR spectrum was used to identify the functional groups present on the carbon spheres after microwave-hydrothermal treatment, as shown in Fig. 1A, curve b. For comparison, the FTIR of glucose was also presented in Fig. 1A, curve a. The decomposition of glucose caused the elimination of many functional groups and led to the formation of gaseous products and coffee-colored, char-like products (Sakaki et al., 1996). The increase in the intensity of the band at 1633 cm^{-1} (C=C) and 1701 cm^{-1} (C=O) for carbon spheres in comparison with glucose supports the idea of aromatization of glucose during the decomposition process. The decrease in the intensity of the bands at 1000–1300 cm^{-1}, including the C–OH stretching and OH bending for carbon spheres, implies the decrease in the hydroxyl groups. Therefore, it seems that the aromatization progresses via a dehydration process. Partially dehydrated residues in which reductive hydroxyl groups (–OH) and aldehyde groups (–CHO) are covalently bonded to the carbon frameworks improve the hydrophilicity and stability of the spheres in aqueous systems, and greatly widen their potential applications in diagnostics and drug delivery (Hans and Lowman, 2002). Furthermore, the original colloidal carbon spheres in water had a negative ζ-potential of −30.5 mV, indicating the existence of many –COOH groups, which could be used to covalently combine with Ab molecules. The narrow size distributions of the products were demonstrated by TEM observation. Fig. 1B shows the TEM image of the colloidal carbon spheres with the diameter of ~300 nm. Moreover, following the TEM image, some spheres were found to form hexagonal contacts with one another, and this suggests their potential use in the construction of CSA. Fig. 1C shows the SEM image of the resultant CSA modified ITO, indicating that a single-layered arrangement of carbon spheres with (1 1 1) plane paralleled the substrate surface.

3.2. Characterization of the CSA modified electrode

As the synthetic procedure of the carbon spheres does not involve the use of organic solvents, initiators, or surfactants, the synthesized carbon spheres are 'green', and can be selected as a strong candidate for application in bioassay. After the combination of Ab molecules with the carbon spheres, the number of organic functional groups decreased, as revealed by the FTIR spectrum in Fig. 1A, curve c. The O–H stretching band centered at 3450 cm^{-1} and OH bending vibrations of original carbon spheres were all weakened because of the formation of amido link between Ab and carbon spheres. The former C=O vibration at 1701 cm^{-1} of carbon spheres was now inconspicuous, indicating that carboxyl groups on the spheres reacted almost entirely with amino groups in Ab molecules. The CSA modified electrode was electrochemically characterized in PBS (50 mM, pH 7.4) solution containing 0.1 M KCl and 2 mM $Fe(CN)_6^{3-}/Fe(CN)_6^{4-}$ at a scan rate of 100 mV s^{-1} as shown in Fig. 1D, curve b. For comparison, curve a presented the CV of a glassy carbon electrode (GCE) with the same geometric surface area. Prior to the CV sweep, polished GCE was oxidized at +1.5 V in a mixture solution containing 10% HNO_3 and 2.5% $K_2Cr_2O_7$ for 25 s to make the carbon surface with –COOH groups (Millan and Mikkelsen, 1993). The carboxylation of GCE would create a similar microenvironment of electrode surface as that of CSA. The contrast between these two cyclic voltammograms indicates that the CSA modified electrode has a larger active surface area.

3.3. Electrochemical characteristics of the electrode surface

All electrochemical measurements were performed in a pH 7.4 PBS solution containing 0.1 M KCl and 2 mM $Fe(CN)_6^{3-}/Fe(CN)_6^{4-}$. The CV of ferricyanide was chosen as a marker to investigate the changes of the electrode behavior after each assembly step. Fig. 2A shows the CVs of $Fe(CN)_6^{3-}/Fe(CN)_6^{4-}$ at the CSA modified electrode (curve a), Ab combined electrode (curve b), Ab combined electrode blocked with BSA (curve c), and IgA conjugated electrode (curve d), respectively. As shown in Fig. 2A, stepwise modification at CSA was accompanied by a decrease in the amperometric response and an increase in the peak-to-peak separation between the cathodic and anodic waves of the redox probe, showing that the electron transfer kinetics of $Fe(CN)_6^{3-}/Fe(CN)_6^{4-}$ was obstructed. After Ab, BSA and IgA molecules were immobilized onto the CSA modified electrode in turn, the peak currents of the redox couple of $Fe(CN)_6^{3-}/Fe(CN)_6^{4-}$ decreased successively (curves b–d), because of the insulative properties of these biomolecules. In the controlled experiment, carboxylated GCE was used to fabricate another IgA immunosensor and the production process was similar to that based on CSA. After Ab molecules were combined covalently with –COOH and 3% BSA was used to block the residual active sites on the surface of GCE, the IgA electrochemical immunosensor was obtained to detect the concentration of IgA in the synthetic solutions. Surprisingly, the CV and EIS responses almost overlapped with that of BSA obturated GCE in higher IgA concentrations (Fig. 2C and 2D). This might be ascribed to the small amount of Ab molecules combined on the surface of carboxylated GCE and consequently, the quantity of conjugated IgA might be small, too.

As most antibodies and antigens are electrochemically inert, the label-free technique of EIS is developed to provide a direct detection

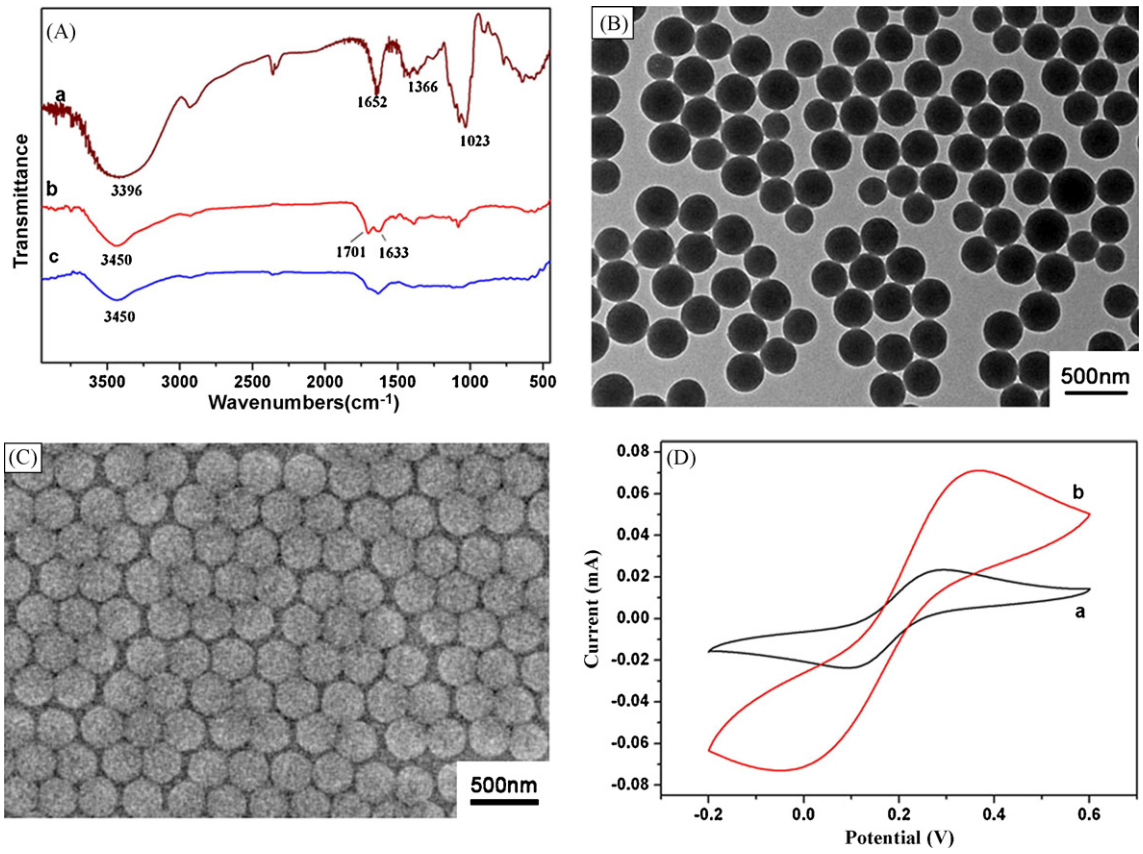

Fig. 1. (A) FTIR spectra of (a) glucose, (b) pure carbon spheres sample, (c) carbon spheres combined with Ab. (B) TEM image of colloidal carbon spheres. (C) SEM image of CSA modified ITO. (D) Cyclic voltammograms of (a) carboxylated GCE, (b) CSA modified electrode recorded in pH 7.4 PBS solution containing 0.1 M KCl and 2 mM $Fe(CN)_6^{3-}/Fe(CN)_6^{4-}$ at 100 mV s^{-1}.

for immunospecies by measuring the change of impedance. Analysis of the system response provides information concerning the electrical behavior of the interface and the interaction occurring on it (Navrátilová and Skládal, 2004). The impedance spectra include a semicircle portion and a linear portion. The semicircle diameter at higher frequencies corresponds to the electron transfer resistance (R_{et}), and the linear part at lower frequencies corresponds to the diffusion process. Fig. 2B shows the EIS of the electrode at different stages. It was observed that the R_{et} of the CSA modified electrode was about 439 Ω (curve a), due to the negatively charged property of the spheres that reduced the ability of the redox probe to access that layer. Subsequently, Ab molecules were covalently combined with CSA and the R_{et} increased again to about 726 Ω (curve b) because of the poor conductivity of Ab molecules. The ζ-potential of Ab combined carbon spheres was also detected as −20.5 mV, illustrating that the surface of the Ab modified electrode electrostatically repelled the redox probe. As the p*I* of BSA was 4.7, BSA was positively charged when prepared in pH 4.0 PBS. The electrostatic attraction between BSA and the Ab modified electrode could promote the blocking of residual active sites on the electrode surface. After the electrode was blocked with BSA, the R_{et} increased significantly to about 1250 Ω (curve c), then to about 1840 Ω by the combination of IgA and Ab (curve d). The reason for this is that the protein on the electrode acted as the inert electron and mass-transfer blocking layer, and they significantly hindered the diffusion of ferricyanide toward the electrode surface. The EIS results were consistent with the CV curves shown in Fig. 2A. In comparison with CV, the results of EIS presented more apparent differences to multilayers deposited on the CSA electrode, indicating better sensitivity.

3.4. Detection of IgA

To evaluate the reaction between Ab and IgA, we exposed the BSA/Ab–CSA modified electrode to various concentrations of IgA, C_{IgA}. The corresponding Nyquist plots of impedance spectra are shown in Fig. 3A, the diameter of the Nyquist circle increasing with the addition of IgA. This may be because more IgA molecules can bind to the immobilized Ab in higher concentrations, which acts as a definite kinetic barrier for the electron transfer. The EIS results can be simulated with an equivalent circuit as shown in the inset of Fig. 3A. The modified Randle's equivalent circuit and the fitting of measured spectra to the equivalent circuit (solid line) are both shown in Fig. 3A, indicating good agreement with the circuit model and the measurement system over the entire measurement frequency range. The equivalent circuit consists of the ohmic resistance (R_s) of the electrolyte solution. The double-layer capacitance (C_{dl}) between electrode and solution is related to the electrode surface condition. Since the surface of the CSA modified electrode was very rough and the electron-transfer impedance was measured in the presence of electroactive probe $Fe(CN)_6^{3-/4-}$, we used a constant phase element (CPE) instead of the classical capacitance to fit the impedance data (Pajkossy, 1994). Electron-transfer resistance (R_{et}) exists when a redox probe is present in the electrolyte solution. Warburg impedance (Z_w) results from the diffusion of ions from the bulk of the electrolyte to the electrode interface. Ideally, the two components R_s and Z_w may represent the bulk properties of the electrolyte solution and the diffusion of the redox probe present in the solution. Thus, they are not affected by chemical transformations at the electrode interface. In the experiments, a negligible change in R_s and Z_w was

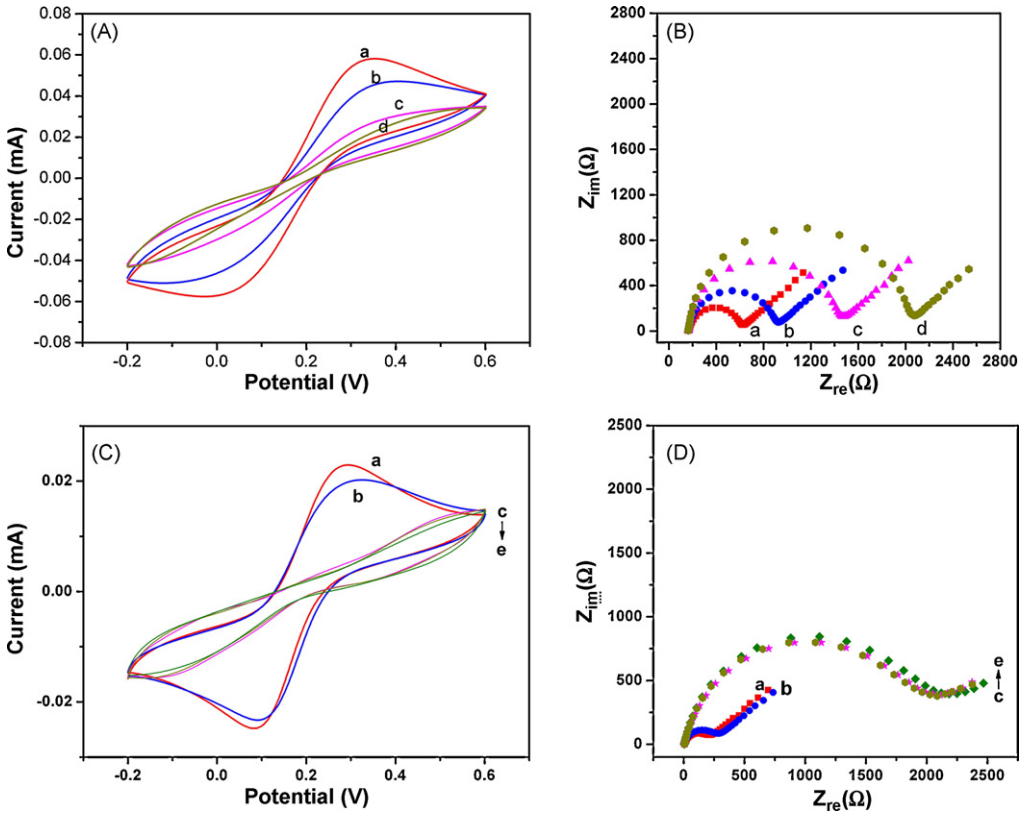

Fig. 2. Upper (A) and (B) were the CV and Nyquist plots of the CSA modified electrode. Lower (C) and (D) were the CV and Nyquist plots of the carboxylated GCE. They were all recorded in PBS (50 mM, pH 7.4) solution containing 0.1 M KCl and 2 mM $Fe(CN)_6^{3-}/Fe(CN)_6^{4-}$. In (A) and (B) (a) CSA modified electrode; (b) Ab combined electrode; (c) BSA blocked electrode; (d) 10 ng mL^{-1} IgA conjugated electrode. In (C) and (D) (a) carboxylated GCE; (b) Ab combined GCE; (c) BSA blocked GCE; (d) 50 ng mL^{-1} IgA conjugated GCE; (e) 150 ng mL^{-1} IgA conjugated GCE. The scan rate was 100 mV s^{-1} and the frequency range of EIS was from 0.01 Hz to100 kHz with signal amplitude of 5 mV.

observed in the modification process. At the same time, as shown in Fig. 3A, the changes in R_{et} were much larger than those in other impedance components. Thus, R_{et} was a suitable signal for sensing the interfacial properties of the immunosensor. The fitted values for the stepwise formation of the multilayers are listed in Table 1.

The change in R_{et} (ΔR_{et}) is calculated by the following equation $\Delta R_{et} = R_{et}(Ag–Ab) - R_{et}(BSA)$, where $R_{et}(Ag–Ab)$ is the value of the electron-transfer resistance after IgA coupling to the immobilized Ab on the CSA electrode. $R_{et}(BSA)$ represents the value of the impedance after blocking the remaining reactive sites by BSA. As can be seen, ΔR_{et} increased with increasing antigen concentrations within the detection range. However, the increases in ΔR_{et} were not obvious at higher antigen concentrations due to steric hindrance or saturation of coupled antigen molecules. The electrochemical IgA immunosensor displayed well-defined concentration dependence. As shown in Fig. 3B, a linear relation between the ΔR_{et} responses and the logarithmic value of antigen concentrations was observed in a range from 0.1 to 200.0 ng mL^{-1}. According to the linear relationship, IgA concentration was detected quantitatively. Higher serum IgA levels could be detected by an appropriate dilution with pH 6.0 PBS.

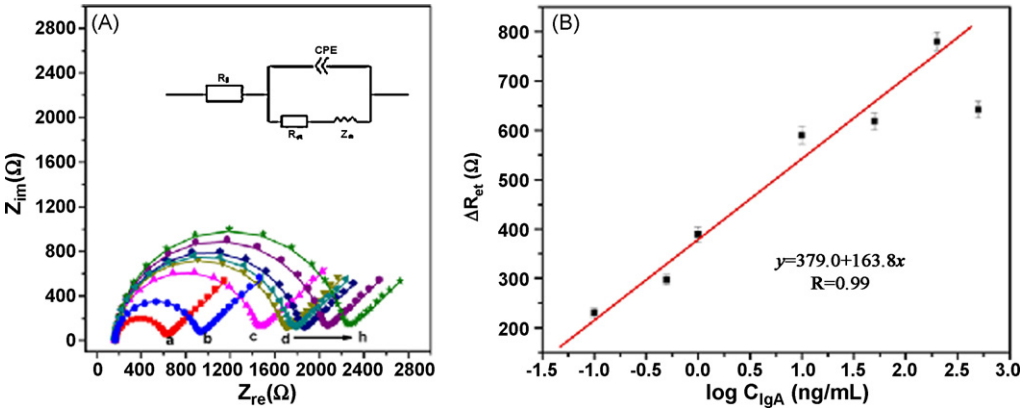

Fig. 3. (A) Fitted (solid line) and experimental (dotted line) Nyquist plots of Faradaic impendence spectra corresponding to the CSA modified electrode before and after incubating with different concentrations of IgA in PBS (50 mM, pH 7.4) solution containing 0.1 M KCl and 2 mM $Fe(CN)_6^{3-}/Fe(CN)_6^{4-}$. Curves (a–c) were same as Fig. 2B; curves (d–h) represent 0.1, 0.5, 1.0, 10.0, and 200.0 ng mL^{-1} IgA, respectively. (Inset) Equivalent circuit for the impedance spectroscopy in the presence of redox probes using a constant phase element (CPE) instead of capacitance. (B) Calibration curve for the IgA immunosensor.

Table 1
Fitting values of the equivalent circuit elements for the IgA immunosensor based on the CSA modified electrode from Fig. 3A.

	R_s (Ω)[a]	CPE (μF)[a]	R_{et} (Ω)[a]	Z_w ($\times 10^{-2}$ Ω)[a]	ΔR_{et} (Ω)
CSA modified electrode	186.4	3.001	439	0.5239	–
Combined with Ab	205.9	3.786	726	0.4961	–
Blocked by BSA	211.9	3.991	1250	0.4343	–
0.1 ng/mL IgA	201.4	3.875	1480	0.5019	230
0.5 ng/mL IgA	211.3	4.106	1547	0.5215	297
1 ng/mL IgA	198.2	4.028	1639	0.5541	389
10 ng/mL IgA	189.5	3.873	1840	0.5259	590
50 ng/mL IgA	184.0	3.934	1868	0.5480	618
200 ng/mL IgA	184.9	3.845	2030	0.5336	780
500 ng/mL IgA	214.0	4.046	1892	0.5467	642

[a] $n = 3$. Measurements were carried out on the 3 independently fabricated electrodes, and the values were average of 3 measurements.

3.5. Specificity, stability and precision of the immunosensor

To further characterize the specificity of the immunosensor, 20 ng mL^{-1} of goat IgA and 10 ng mL^{-1} of IgA were first mixed and then EIS response was detected. In comparison with the EIS response obtained from the pure IgA, no significant difference was observed. The relative standard deviation (RSD) was 5.2%, indicating that the goat IgA could not cause observable interference, and it is thus feasible to use the immunosensor for the determination of IgA in serum. The inter-assay precision was estimated by determining the IgA level with three immunosensors of different batches under the same experimental conditions. The RSD of the inter-assay was 4.8% at the IgA concentration of 10 ng mL^{-1}, indicating acceptable precision and fabrication reproducibility. The immunosensor retained its EIS and CV response after 60 days in air at 4 °C, without obvious decline. This indicates that the CSA modified electrode is efficient to retain the bioactivity of antibodies. Simultaneously, because of the covalent interaction between CSA and immobilized Ab, it could also prevent the leakage of Ab molecules.

3.6. Application of the immunosensor in human serum

The feasibility of the immunoassay system for clinical applications was investigated by analyzing several real samples, in comparison with the ELISA method. These serum samples were diluted to different concentrations with PBS of pH 6.0. Fig. 4 describes the correlation between the results obtained by the proposed IgA immunosensor and the ELISA method. This indicates that there is no significant difference between our results and the ELISA tests. Therefore, the developed immunosensor could be satisfactorily applied to the clinical determination of IgA levels in human serum.

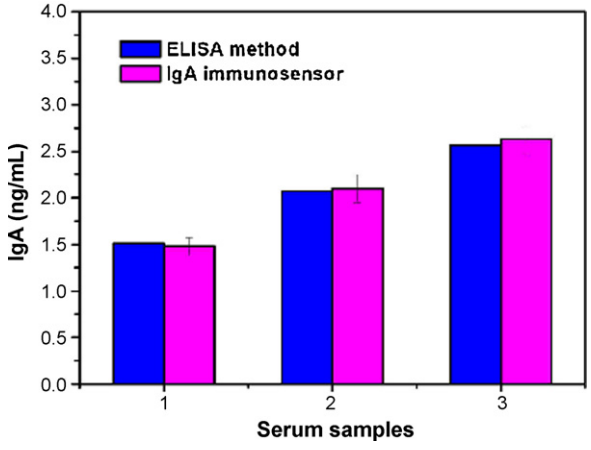

Fig. 4. Comparison of serum IgA levels determined using IgA immunosensor and ELISA method.

4. Conclusion

We have developed a novel method for the fabrication of disposable EIS immunosensor based on the CSA modified electrode that is both efficient and convenient. The as-prepared CSA modified electrode may not only maintain the advantage of carbon spheres, such as conductivity, stability, biocompatibility and reactivity, but also facilitate the covalent immobilization of antibody molecules directly. The immunodetection of IgA both in synthetic and real samples indicated that the CSA might be useful as a biocompatible platform for future sensitive biosensing.

Acknowledgements

We greatly appreciate the support of the National Natural Science Foundation of China (20635020, 20821063 and 20605011). This work is also supported by National Basic Research Program of China (2006CB933201 and 2007CB936404).

References

Arumugam, P.U., Chen, H., Siddiqui, S., Weinrich, J.A.P., Jejelowo, A., Li, J., Meyyappan, M., 2009. Biosens. Bioelectron. 24, 2818–2824.
Bakker, E., Qin, Y., 2006. Anal. Chem. 78, 3965–3984.
Cui, R.J., Huang, H.P., Yin, Z.Z., Gao, D., Zhu, J.J., 2008a. Biosens. Bioelectron. 23, 1666–1673.
Cui, R.J., Liu, C., Shen, J.M., Gao, D., Zhu, J.J., Chen, H.Y., 2008b. Adv. Funct. Mater. 18, 2197–2204.
Fu, X.H., 2007. Electroanalysis 19, 1831–1839.
Fu, Z.F., Hao, C., Fei, X.Q., Ju, H.X., 2006. J. Immunol. Methods 312, 61–67.
Gonzalez-Martinez, M.A., Puchades, R., Maquieira, A., 1999. TrAC, Trends Anal. Chem. 18, 204–218.
Hans, M.L., Lowman, A.M., 2002. Curr. Opin. Solid State Mater. Sci. 6, 319–327.
He, P.L., Wang, Z.Y., Zhang, L.Y., Yang, W.J., 2009. Food Chem. 112, 707–714.
Jie, G.F., Zhang, J.J., Wang, D.C., Cheng, C., Chen, H.Y., Zhu, J.J., 2008. Anal. Chem. 80, 4033–4039.
Jin, X.Y., Jin, X.F., Chen, L.G., Jiang, J.H., Shen, G.L., Yu, R.Q., 2009. Biosens. Bioelectron. 24, 2580–2585.
Krishnamoorthy, S., Iliadis, A.A., Bei, T., Chrousos, G.P., 2008. Biosens. Bioelectron. 24, 313–318.
Li, J., Papadopoulos, C., Xu, J.M., Moskovits, M., 1999. Appl. Phys. Lett. 75, 367–369.
Lin, J.H., Ju, H.X., 2005. Biosens. Bioelectron. 20, 1461–1470.
Luijkx, G.C.A., van Rantwijk, F., van Bekkum, H., Antal Jr., M.J., 1995. Carbonhydr. Res. 272, 191–202.
Maldonado, S., Stevenson, K.J., 2004. J. Phys. Chem. B 108, 11375–11383.
Mani, V., Chikkaveeraiah, B.V., Patel, V., Gutkind, J.S., Rusling, J.F., 2009. ACS Nano 3, 585–594.
Marquette, C.A., Blum, L.J., 2006. Biosens. Bioelectron. 21, 1424–1433.
Millan, K.M., Mikkelsen, S.R., 1993. Anal. Chem. 65, 2317–2323.
Navrátilová, I., Skládal, P., 2004. Bioelectrochemistry 62, 11–18.
Nguyen, C.V., Delzeit, L., Cassell, A.M., Li, J., Han, J., Meyyappan, M., 2002. Nano Lett. 2, 1079–1081.
Orikasa, H., Akahane, T., Okada, M., Tong, Y., Ozaki, J., Kyotani, T., 2009. J. Mater. Chem. 19, 4615–4621.
Pajkossy, T.J., 1994. Electroanal. Chem. 364, 111–124.
Rahman, S., Yang, H., 2003. Nano Lett. 3, 439–442.
Sakaki, T., Shibata, M., Miki, T., Hirosue, H., Hayashi, N., 1996. Bioresour. Technol. 58, 197–202.
Sanchez-Martinez, M.L., Aguilar-Caballos, M.P., Gomez-Hens, A., 2007. Anal. Chem. 79, 7424–7430.
Suni, I.I., 2008. TrAC, Trends Anal. Chem. 27, 604–611.

Viswanathan, S., Rani, C., Anand, A.V., Ho, J.A., 2009. Biosens. Bioelectron. 24, 1984–1989.
Wang, J., Lin, Y.H., 2008. TrAC, Trends Anal. Chem. 27, 619–626.
Wang, Q., Li, H., Chen, L.Q., Huang, X.J., 2002. Solid State Ionics 152–153, 43–50.
Watterson, J.M., Stallcup, P., Escamilla, D., Chernay, P., Reyes, A., Trevino, S.C., 2007. J. Clin. Lab. Anal. 21, 162–166.
Withey, G.D., Lazareck, A.D., Tzolov, M.B., Yin, A., Aich, P., Yeh, J.I., Xu, J.M., 2006. Biosens. Bioelectron. 21, 1560–1565.
Wu, L.N., Yan, F., Ju, H.X., 2007. J. Immunol. Methods 322, 12–19.
Yun, Y.H., Shanov, V., Schulz, M.J., Dong, Z., Heineman, W.R., Hasall, H.B., Wong, D.K.Y., Bange, A., Tu, Y., 2007. J. Nanosci. Nanotechnol. 7, 891–897.
Yun, Y.H., Dong, Z.Y., Shanov, V.N., Doepke, A., Heineman, W.R., Halsall, H.B., Bhattacharya, A., Wong, D.K.Y., Schulz, M.J., 2008. Sens. Actuators B 133, 208–212.
Zacco, E., Adrian, J., Galve, R., Marco, M.P., Alegret, S., Pividori, M.I., 2007. Biosens. Bioelectron. 22, 2184–2191.